5 Modeling surface processes

5.1 Background

The surface processes whose numerical simulation is discussed here occur near both the land–atmosphere and the water–atmosphere interfaces. Over land, the movement of heat and water within the plant canopy and the ground beneath it must be represented in both weather- and climate-prediction models. Through this movement of heat and water across the land–atmosphere interface, properties of the land surface such as temperature and wetness are felt by the atmospheric boundary layer and the free atmosphere above. The atmosphere, in turn, affects the substrate and vegetation properties through radiation, precipitation, and controls on evapotranspiration. The effect of the surface on the frictional stress felt by the air moving over it is more the subject of boundary-layer meteorology and parameterizations rather than land-surface physics, so most of the discussion of this topic is found in Chapter 4. Over water, the interaction is complicated by the fact that the wind stress causes currents, waves, and vertical mixing of the water, which affect surface temperature and evaporation.

The skillful numerical prediction of atmospheric processes of many types and scales depends on the proper representation of surface–atmosphere interactions. For example, the prediction of convection relies on the accurate calculation by the model of surface fluxes of heat and water vapor. And, direct thermal circulations on the mesoscale, forced by horizontally differential heating at the surface, can dominate the local weather and climate near coastlines and sloping orography. On larger scales, monsoon circulations respond to seasonal variations in surface-heating differences between continents and oceans. And the modification of air masses by surface–atmosphere heat fluxes is an important factor that controls near-surface temperatures on the synoptic scale. On the global scale, the processes associated with the ENSO cycle involve ocean–atmosphere interaction. Indeed, of course the entire general circulation of the atmosphere is driven by differential surface heating, and a critical link in the global hydrologic cycle is the evapotranspiration at the surface. There are many more examples of atmospheric phenomena whose accurate simulation or forecasting depends on skillfully modeling the surface–atmosphere interaction, and the subsurface processes, over land and water.

Although many similar land-surface processes prevail on both weather and climate time scales, there are some that are only important for climate forecasting. Examples of these include interactions related to the carbon cycle, as well as changes in plant species associated with drought and other climate change. Modeling both categories of processes will be

considered in this chapter, although the climate-related ones are discussed in greater detail in Chapter 16.

Because most students and professionals who are studying NWP will not have had the same background in land and ocean processes as they have had in atmospheric dynamics and thermodynamics, a summary is offered here in order to illustrate what must be included in a complete model. More detail will be provided below about land processes relative to ocean processes because, on weather-prediction time scales of a week or two, it is typical to assume that water conditions (e.g., temperature) are constant. In contrast, because of the fast response of the land conditions to precipitation, diurnal and day-to-day variations in solar radiation, frontal passages, etc., land-surface and subsurface processes are modeled explicitly or parameterized in virtually all models.

There are two ways in which Land-Surface Models (LSM) are used in NWP. They are integral components of the atmospheric model, and are run simultaneously with the rest of the code to predict or simulate surface fluxes of heat, moisture, and momentum. And, they are used as the basis of Land Data-Assimilation Systems (LDAS), which are run as stand-alone systems that ingest observed meteorological variables in order to diagnose current substrate temperature, moisture, and vegetation conditions for use in model initialization. That is, the LDAS is not coupled with the atmospheric model when it is run.

There is a hierarchy of LSMs that are appropriate for different applications, and all the processes discussed here do not need to be represented in every LSM. Nevertheless, regardless of the level of complexity of the treatment, the surface-process representations are an integral part of the atmospheric-model code. Thus, it is important for the model user to understand the strengths and weaknesses of this part of the model, just as with any other aspect of the model – just because it is not atmospheric science does not mean that LSMs can be treated as black boxes.

5.2 Land-surface processes that must be modeled

Land-surface models use atmospheric information (wind speed, temperature, etc.) from the atmospheric model's surface-layer representation, precipitation forcing from the convective and microphysics parameterizations, and radiative forcing from the radiation scheme. This forcing is used with information about the land's state variables to calculate the surface fluxes of heat and moisture to the atmosphere, reflected shortwave radiation, and longwave radiation emitted to the atmosphere and space. An appreciation for the breadth of the topic of land-surface processes and modeling can be developed through Fig. 5.1, which shows the various prevailing physical processes. The processes involve heat transfers, and the movement and transformation of water in its various forms. Within the substrate, there are the following processes.

- Liquid water is transported downward through gravity drainage and in all directions through capillary effects. Water also can rise and fall through changes in the water table.
- Water vapor moves vertically through the air spaces by convection and molecular diffusion.

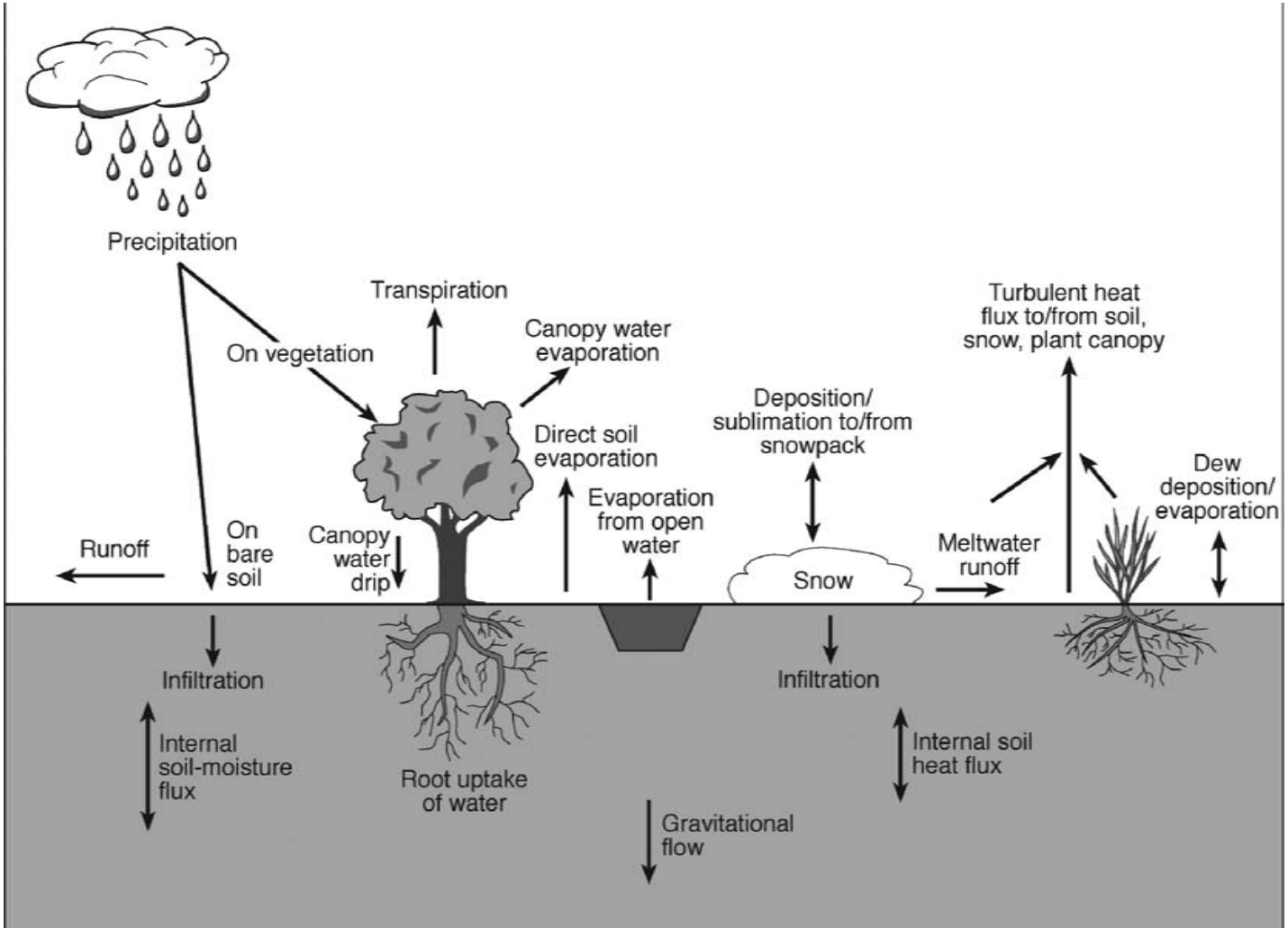

Fig. 5.1 Schematic showing physical processes that are associated with the movement of heat and water within the substrate and at the surface. Adapted from Chen and Dudhia (2001).

- The roots of vegetation draw water from the substrate within the root zone.
- The substrate water freezes and thaws, with the release and consumption of the latent heat of fusion.
- Evaporation and condensation occur, with the release and consumption of the latent heat of condensation.
- Heat is conducted.

At the interface between the substrate surface and the atmosphere, there are the following exchanges.

- Rainwater, snowmelt water, irrigation water, and dew enter the substrate.
- Water from the substrate evaporates and sublimates into the atmosphere.
- Heat is exchanged between the atmosphere and the substrate.
- Liquid water passes from the underground roots to the above-ground stems and leaves.

Immediately above the interface, the following processes are important.

- Rain falls on the bare ground and vegetation.
- Water drips from vegetation onto the bare ground or onto other vegetation.
- Snow accumulates on the bare ground and vegetation.
- Snow and frost melt and sublimate, consuming heat.
- Dew and frost form on the bare ground and vegetation, releasing latent heat.
- Fog deposits on the bare ground and vegetation.
- Water evaporates from the leaf surfaces of vegetation, and transpires from vegetation, with the consumption of heat.

5.2.1 The energy and water budgets of the land surface

The energy and water budgets at the land surface control the temperature and moisture content of the substrate and vegetation, which interact with the atmosphere. The energy-conservation equation can be written for a unit mass or unit area of the surface that is experiencing gains or losses of energy:

$$R = LE + H + G \tag{5.1}$$

The variable R is the net radiation, L is the latent heat of evaporation, E is the evaporation or condensation rate, H is the sensible-heat exchange between the substrate/vegetation and the atmosphere, and G is the sensible-heat exchange (conduction) between the surface and the subsurface substrate. The quantity LE is the latent-heat flux, and H and G are heat fluxes also, all with the same dimensions as R. The net radiation represents the rate of radiant energy gain or loss at the surface of Earth, after accounting for all the various sources and sinks of short- and longwave radiation. The surface radiative energy balance is symbolically represented as

$$R = (Q + q)(1 - \alpha) - I\uparrow + I\downarrow, \tag{5.2}$$

where R is the net radiation, Q is the direct-solar and q is the diffuse-solar radiation incident on Earth's surface, α is the surface albedo, $I\uparrow$ is the outgoing longwave radiation

from the surface, and $I\downarrow$ is the absorbed downwelling longwave radiation that has been emitted by the atmosphere (gas, particulates, and clouds). Equation 5.1 simply states that the radiative energy gain or loss at the surface, R, must equal the sum of the other three terms. During the day, the rate of energy gain at the surface must equal the loss of energy associated with evaporation, the loss associated with heat conduction away from the surface into the substrate, and the loss of sensible heat to the atmosphere.

The water budget for a shallow soil layer at the surface can be represented as

$$\frac{\partial \Theta}{\partial t} = P - ET - RO - D, \tag{5.3}$$

where Θ (dimensionless) is the volumetric soil water content; P is the rate of input through precipitation, snowmelt, dew and fog deposition, and irrigation water; ET is the rate of loss through evapotranspiration; RO is the rate of loss through lateral runoff; and D is the rate at which water is lost through drainage to deeper layers.

5.2.2 Vertical heat transport within the substrate

Vertical heat transport within substrates is mostly through conduction (i.e., molecular diffusion), even though convective and advective movement of air can transport heat when the porosity (percentage air space) is high. This subsurface transport is important because it strongly modulates the thermal-energy budget at the surface. For example, heat gained and stored by the substrate during the day can be released to the atmosphere at night, affecting the boundary-layer structure and moderating the nocturnal minimum temperatures.

Because the substrate is a medium potentially consisting of solid, liquid, and gas phases, the thermal conductivity will depend on the proportions and characteristics of these components. The direction of the conductive heat transfer is from higher temperature to lower temperature, and the magnitude of the heat flux is proportional to the temperature gradient. Mathematically,

$$H_s = -k_s \frac{\partial T_s}{\partial z}, \tag{5.4}$$

where H_s is the heat flux in the soil (positive upward), k_s is the soil thermal conductivity, z is distance on the vertical axis (positive upward), and T_s is the substrate temperature. That is, the heat flux is proportional to the temperature gradient multiplied by a factor that reflects the ability of the substance to transfer heat. This is called a flux-gradient form of equation. The negative sign indicates that the flux is in the direction of lower temperature. The thermal conductivity is formally defined as the quantity of heat that flows through a unit cross-sectional area per unit time, when there exists a temperature gradient of one degree per unit distance perpendicular to the cross section. In general, a soil consists of solid substrate particles, liquid water, ice, and air spaces, and the relative contributions from the conductivity of these four components determines the total soil conductivity. The existence of water in the soil dramatically increases the thermal conductivity, not only because the conductivity of water is high, but because the water displaces the air which

has an especially low conductivity (i.e., air is a good thermal insulator). Specifically, the conductivity of air is about two orders of magnitude lower than that of rock or wet soil. Thus, tabulated values of conductivity should specify the soil-moisture content and the porosity of the soil. Figure 5.2 shows qualitatively how the conductivity and other thermal properties of soil depend on the soil-moisture content.

Another important physical property of a substrate is the thermal, or heat, capacity, which describes how much heat is required to raise the temperature of a unit volume by one degree. As with the conductivity, the value of the soil heat capacity (C_s) depends on the fractions of the soil solids, liquid water, ice, and air. Air has a low heat capacity, so displacing air with water, as soil is moistened, raises the heat capacity of the air–water–solid mixture (Fig. 5.2b). Thus, more heat is required to raise the temperature of a moist soil than a dry soil. A related quantity is the specific heat (c), which is the amount of heat required to raise the temperature of a unit mass by one degree. Thus, it is equal to the heat capacity divided by the density of the substrate ($c = C/\rho$). The heat capacity and the specific heat are sometimes referred to as the soil's thermal sensitivity.

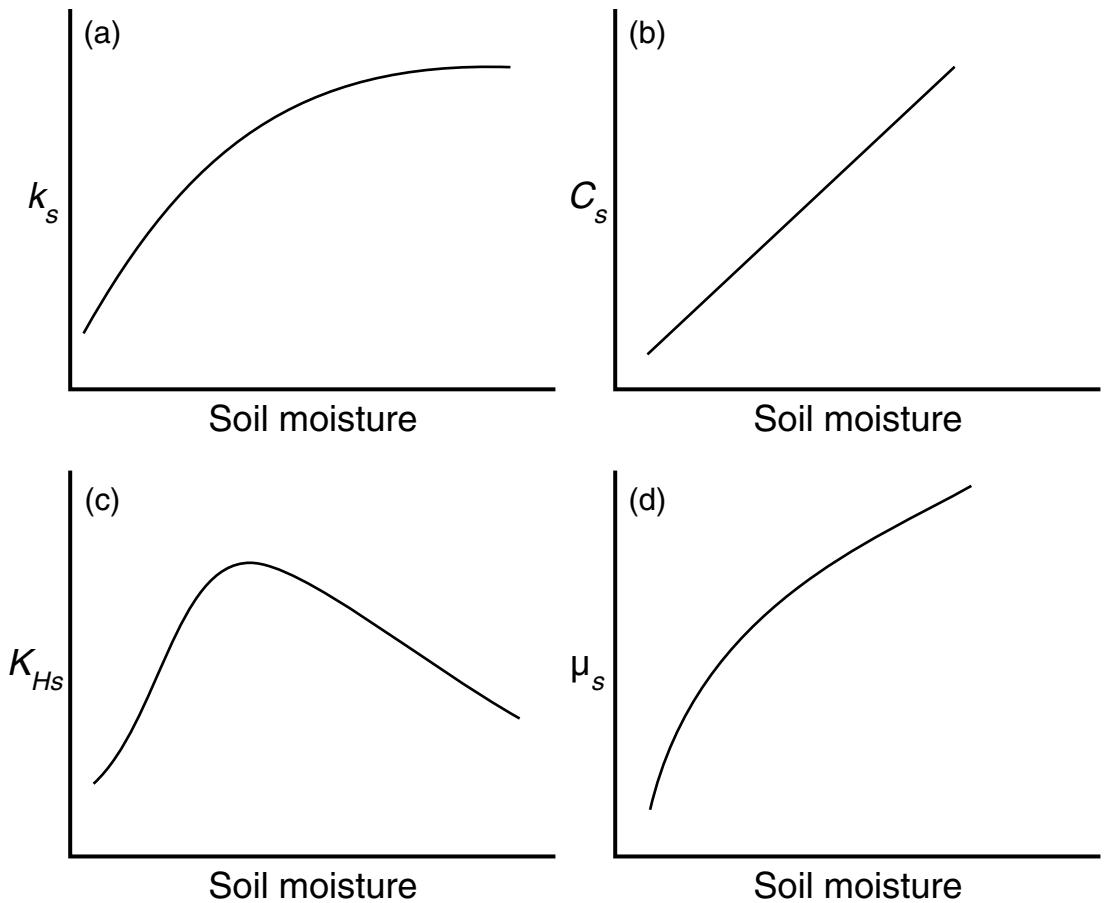

Fig. 5.2 General relationship between soil-moisture content and (a) thermal conductivity, (b) heat capacity, (c) thermal diffusivity, and (d) thermal admittance for most soils. From Oke (1987).

A quantity that is related to the heat capacity and the thermal conductivity is the thermal diffusivity ($K_{Hs} = k_s/C_s$). We will see that it determines the speed with which a temperature change propagates through a medium such as soil. Imagine the surface of the substrate heating up during the daytime heating cycle, which creates an upward temperature gradient immediately below the surface. Equation 5.4 predicts a downward heat flux that is directly proportional to the soil's thermal conductivity. Because the temperature gradient and therefore the heat flux are still small some distance below the surface, there will be a heat-flux convergence between the surface and that level. That is, the downward heat flux into the layer from the top is greater than the downward heat flux out of the layer at the bottom. This will raise the temperature of the soil in the layer in inverse proportion to its heat capacity, as shown in Eq. 5.5:

$$\frac{\partial T_s}{\partial t} = -\frac{1}{C_s}\frac{\partial H_s}{\partial z}. \tag{5.5}$$

In the above example, H_s just below the surface has a large negative value, and is less negative with greater depth. The vertical derivative is thus negative, providing for a temperature increase. Combining Eqs. 5.4 and 5.5 gives

$$\frac{\partial T_s}{\partial t} = \frac{1}{C_s}\frac{\partial}{\partial z}\left(k_s\frac{\partial T_s}{\partial z}\right) = \frac{k_s}{C_s}\frac{\partial^2 T_s}{\partial z^2} = K_{Hs}\frac{\partial^2 T_s}{\partial z^2}, \tag{5.6}$$

where the simplification has been made that k_s does not vary with depth. Here we see that the rate of temperature change is proportional to the diffusivity and the second derivative of temperature with respect to depth. Figure 5.3 shows a schematic of an idealized temperature distribution immediately above and below the air–ground interface, for both nighttime and daytime conditions. During the day, the curvature of the temperature profile below the surface is such that the second derivative in Eq. 5.6 is positive and the temperature increases. When the curvature reverses at night, the substrate cools. Note that a constant rate of temperature change with depth (a straight, sloping line in Fig. 5.3) would produce the same flux everywhere (Eq. 5.4), and no temperature change (Eq. 5.5).

Figure 5.2 shows that diffusivity is directly proportional to soil moisture, for low soil moisture, because the conductivity increases faster with increasing soil moisture than does the heat capacity. When the conductivity curve develops less slope than does the heat-capacity curve at higher soil moistures, the diffusivity begins to decrease.

Another way of understanding how the diurnal temperature wave at and below the surface is related to substrate properties is through the concept of thermal admittance, which is a property of the interface between two media (e.g., the substrate and the atmosphere). It is defined as $\mu_s = (k_s C_s)^{1/2}$, and is a measure of the ability of a surface to accept or release heat. Consider your feet in contact with a tile floor that has a temperature that is lower than your skin temperature. The temperature gradient at the skin–tile interface causes a flux from you to the tile, and a critical factor that determines whether the surface "feels" cold to you is whether the tile surface warms very rapidly to your skin temperature, or whether it remains colder. In the case of the tile, the conductivity is large so that the heat it gains

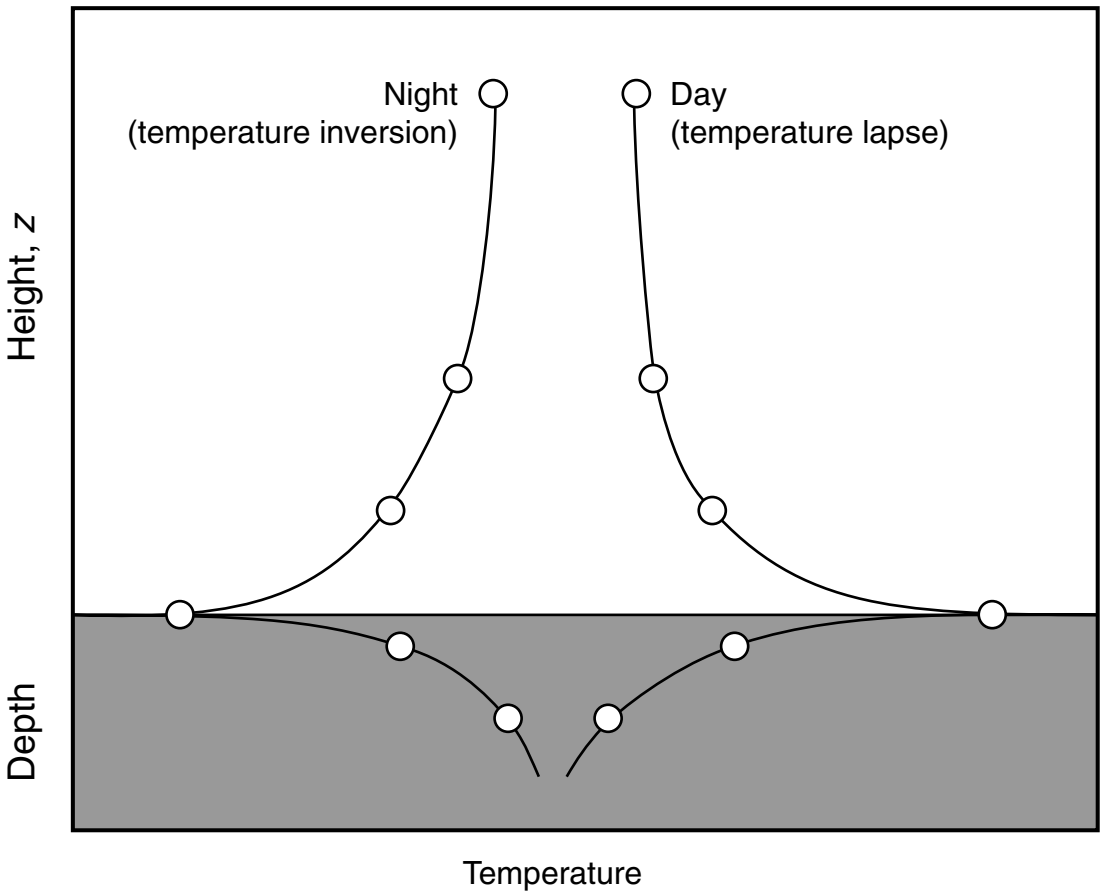

Fig. 5.3 Idealized vertical profiles of temperature in the soil and the atmosphere near the surface. Adapted from Oke (1987).

from your body is conducted rapidly from the surface to the tile material below. Thus, the surface temperature does not rise rapidly, as it would if you were standing on a wood floor having a lower conductivity (i.e., wood is a better thermal insulator). Analogously, if the material has a high heat capacity, its temperature is not going to rise rapidly in response to heat input from your skin. Thus, high conductivity and high heat capacity (i.e., large admittance) contribute to sustaining a large heat transfer across an interface because the temperature contrast is maintained. Of course, the temperature response of the second medium is equally important, so in the case of the surface–air interface, the admittance of the air must also be considered.

Thus, when the surface in contact with the atmosphere has high admittance (i.e., high conductivity and/or high heat capacity), the temperature of the surface does not increase as much during the daytime as it would for a low-admittance surface. This has implications for the daytime surface-energy budget in terms of smaller sensible-heat fluxes to the atmosphere (a cooler boundary layer) and weaker longwave emission from the ground.

The amplitude and time lag of the temperature wave that propagates downward into the substrate during the day also depend on the conductivity and the specific heat. The amplitude

of the daily temperature oscillation is greater for large conductivities and for small heat capacities. That is, the amplitude is proportional to the diffusivity, $K_{Hs} = k_s/C_s$, such that

$$(\Delta T_s)_z = (\Delta T)_0 e^{-z(\pi/K_{Hs}P)^{1/2}}, \tag{5.7}$$

where z is the depth below the surface, P is the wave period (24 h is the dominant period in this discussion of the diurnal temperature wave), $(\Delta T)_0$ is the amplitude of the temperature wave at the surface ($z = 0$), and $(\Delta T_s)_z$ is the amplitude at depth z. That is, the amplitude of the diurnal temperature oscillation decreases exponentially with depth. Figure 5.4a shows

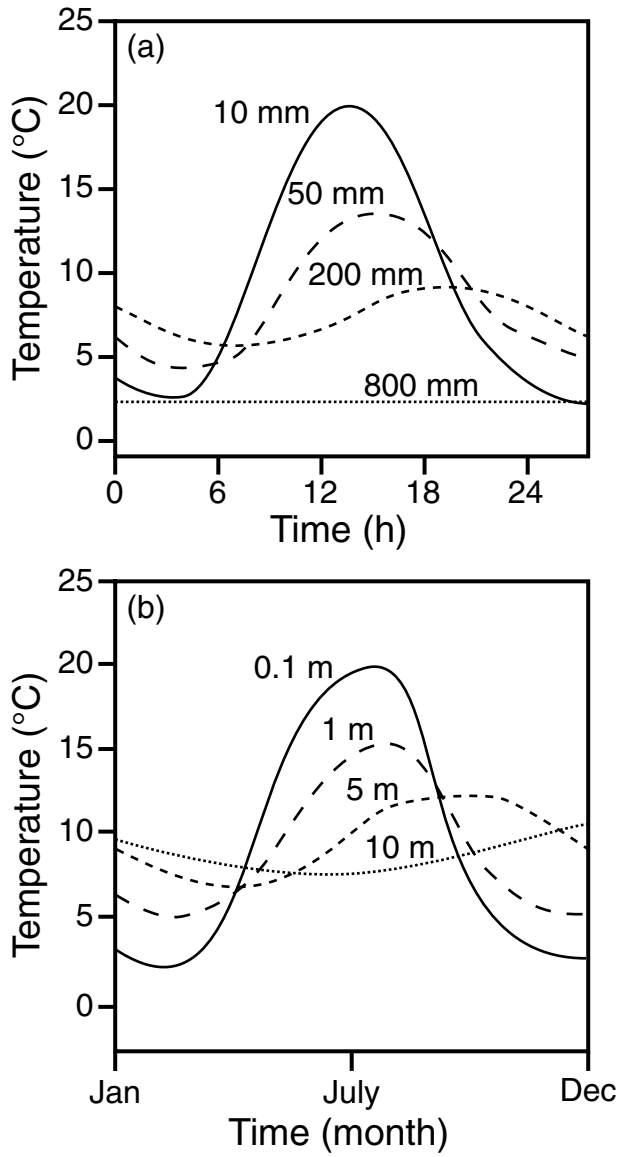

Fig. 5.4 Idealized (a) diurnal and (b) annual cycles of temperature at different depths within the substrate. From Oke (1987).

idealized diurnal temperature variations at different depths on a cloudless day. The time lag with depth shown in the figure is defined by

$$(t_2 - t_1) = \frac{(z_2 - z_1)}{2}(P/\pi K_{Hs})^{1/2}, \tag{5.8}$$

where t_1 and t_2 are the times that a temperature-wave maximum or minimum reaches levels z_1 and z_2, respectively. In other words, the difference is the time required for the temperature wave to pass from one depth to the other. Other variables have the same definition as before. The temperature wave travels faster in substrates with higher thermal conductivity and with lower heat capacity. The time lag means that the near-surface substrate can be cooling while warming continues a short distance below. At some depth, the curves are out of phase so that the time of the temperature maximum at that depth corresponds to the temperature minimum at the surface. Equations 5.7 and 5.8 apply also to the annual cycle, where the period corresponds to that of the seasonal rather than the diurnal cycle (Fig. 5.4b). Equation 5.7 shows that, with a period of 365 days, the depth to which the thermal wave penetrates is about 14 times greater than for the diurnal period (for the same $(\Delta T)_0$). If the diurnal thermal wave penetrates to 0.5 m with a particular amplitude, the annual wave will penetrate to 7 m with the same amplitude.

5.2.3 Vertical water transport within the substrate

There are two general ways for liquid water to enter the substrate between the water table and the surface. Water can move upward from the water table through capillary action (or the water table itself can rise). And, water can enter the substrate from the surface, where this process is called infiltration. The efficiency of infiltration depends on a number of factors such as rainfall intensity, total rainfall amount during a storm, the physical composition of the substrate, and antecedent precipitation. This rate of water movement into the substrate is important because it determines the potential for runoff and flooding, the amount of water near the surface that is available for evaporation, the availability of water for plants, and the extent of groundwater replenishment.

The upward and downward water transport within soils can take place through five mechanisms: Three apply to liquid water and two to water vapor. For liquid water, there are two forces that operate. One is gravity and the other is related to the surface tension between the soil particles and the water. It perhaps seems unusual to refer to surface tension as a force, but molecules at the surface of a liquid experience molecular forces that are not symmetrical and, therefore, not balanced like those experienced by molecules in the fluid's interior, away from the surface. Consider that a volume of soil (or, more familiarly, a sponge) will not drain completely dry after being wetted. Eventually, the drainage rate will approach zero because surface-tension forces, which promote retention of water within the soil (or sponge), balance the gravity force.

In the first mechanism, liquid water can move vertically as a result of a change in the pressure head, which causes the water table to change. That is, a water surface must be in dynamic equilibrium with its surrounding fluid, so local water excesses or deficits

compared to surroundings are reconciled through water movement that equalizes the pressure. A simple illustration of this effect is found in desert environments where a hydrologically closed basin, perhaps containing a salt flat, is surrounded by mountains. Rainfall and snowmelt over the mountains refresh the water table below, which increases the water pressure and causes the groundwater to move laterally (from high to low pressure) into the central basin until equilibrium is attained with a higher water table there. In these situations, frequently the water table reaches the surface, creating seasonal lakes over the salt flats, which should be represented in a model. Analogously, extraction of water at a well site decreases the pressure there and causes inflow from the surroundings, lowering the water table over a wider area. This movement of water in response to pressure differences is forced by gravity; that is, the force of gravity is responsible for static pressure within a fluid. (Static pressure is related to the weight of the fluid above a point, whereas dynamic pressure is a result of fluid movement.)

Second, liquid water can move through soils by capillary action. This movement results from surface-tension effects between the water and soil particles. For example, water can move from the water table into the dry layer above through capillary effects. The capillary-rise layer has a lower bound at the water table and an upper bound that depends on soil properties. In general, capillary effects contribute to the spread of water from wetter to dryer soil. These surface-tension forces that bind the water to the soil particles are determined by the soil porosity and the soil moisture itself. The more porous the soil and the more dry the soil, the weaker are the surface-tension effects. For example, capillary movement of water can be blocked by a layer of open-textured soil (e.g., coarse sand or gravel) or by a dry layer of soil.

Third, downward liquid-water transport between the substrate particles is forced by gravity, where this water is supplied through infiltration – the entry at the surface of water from rain, snowmelt, or irrigation. The infiltration rate is limited by the rate of soil-water movement below the surface, called percolation, with any excess running off laterally or ponding at the surface. The correct modeling of this type of soil-water movement is important to the prediction of groundwater recharge; the evaporation rate; runoff, erosion, and flood production; the availability of water for plant uptake; and chemical changes such as salinization. The rate of this downward water movement, defined as the hydraulic conductivity, is controlled by the surface-tension effects between the soil particles and the water. The force of gravity draws the water downward, but surface-tension forces between the water and soil particles promote retention of the water. This latter effect of water retention is quantified in terms of the soil-moisture potential, which can be visualized as the amount of energy necessary to extract water from the soil matrix. Tight soils, such as clay, have a high potential, or water-retention capacity, compared to sand. Also, dry soils have a higher potential than wet soils: i.e., it takes less energy to extract a unit of moisture from a wet soil than from the same soil after it has become drier. Thus, the hydraulic conductivity is greater when the soil is wet and porous.

The amount of liquid water in soils is generally defined in terms of the soil-moisture content, which is the percentage of the volume of a soil that is occupied by water. The upper limit of the soil-moisture content is determined by the porosity. Coarse-textured soils, such sand, tend to be less porous than fine-textured soils, even though the mean pore

size is greater in the former. The temporal change in the soil-moisture content at any point in a soil can be represented by an equation that is similar to Eq. 5.5, which expresses the local temperature change in terms of the difference in the vertical heat fluxes into and out of a layer (as represented for a point by the vertical derivative of the flux). Analogously, for soil moisture the vertical derivative of liquid-water fluxes must be represented. If the soil-moisture flux toward a point is greater than the flux away from it, the soil moisture increases, and vice versa. The following equation expresses local changes with time in volumetric soil-water content (Θ) as a result of vertical variations in the vertical volume flux of liquid water (q). Note that this expression applies for vertical water transport within subsurface layers, and thus there are no direct effects of sources and sinks of water from precipitation, evaporation, and runoff (as there are for Eq. 5.3, which applies to the surface layer). However, the loss by canopy transpiration of water taken from the root zone is represented by E_t. The term $D_\Theta \partial\Theta/\partial z$ is associated with capillary (i.e., surface tension) water movement and K_Θ represents gravity-forced water movement. These are the second and third mechanisms described above, respectively.

$$\frac{\partial \Theta}{\partial t} = -\frac{\partial q}{\partial z} + E_t = \frac{\partial}{\partial z}\left(K_\Theta + D_\Theta \frac{\partial \Theta}{\partial z}\right) + E_t = \frac{\partial K_\Theta}{\partial z} + \frac{\partial}{\partial z}\left(D_\Theta \frac{\partial \Theta}{\partial z}\right) + E_t . \qquad (5.9)$$

Here, K_Θ is hydraulic conductivity and D_Θ is soil-water diffusivity. The subscripts on K and D refer to their dependence on Θ. The terms conductivity and diffusivity have been borrowed from the equations for the molecular diffusion and conduction of heat, which have terms similar in form to those above. Unfortunately, this terminology does not reflect the actual physical processes that are represented in the equation. The hydraulic conductivity and soil-water diffusivity are highly nonlinearly dependent on the soil moisture (Chen and Dudhia 2001), and have been calculated using various mathematical expressions. For example, Ek and Cuenca (1994) use

$$K_\Theta = K_{\Theta s}(\Theta/\Theta_s)^{2b+3}, \text{ and} \qquad (5.10)$$

$$D_\Theta = -(bK_{\Theta s}\Psi_s/\Theta)(\Theta/\Theta_s)^{b+3}, \qquad (5.11)$$

where $K_{\Theta s}$ is the saturation hydraulic conductivity, Θ_s is the saturation volumetric soil-moisture content, Ψ_s is the saturation soil-moisture potential (a negative number), and b is an empirically defined coefficient. All of these quantities are functions of the soil type.

Why does the temperature need to decrease faster than the dry adiabatic lapse rate?

The above mechanisms apply to liquid-water movement. However, there are also two mechanisms by which water vapor can move vertically above the water table through porous, dry soil: convection and vapor diffusion. Convection requires that the temperature of the soil, and that of the air within the soil, decrease upward in the soil more rapidly than the dry adiabatic lapse rate that is required for the triggering of buoyant motion. The flux of water by vapor diffusion is proportional to the gradient of the water-vapor content of the air within the soil, and results in water vapor transport from areas of higher to lower concentration, without the need for any movement of air on scales larger than the molecular.

5.2.4 Liquid-water transport within vegetation, and transpiration

Vegetation is important to the moisture budget because the roots access shallow and deep moisture that is not otherwise directly available for evaporation at the surface. This moisture is transferred through the xylem up the stems to the leaves, where it evaporates within the intercellular spaces of the leaves and is released through the stomata into the atmosphere. The latent heat consumed in this process is provided by the foliage, in contrast to evaporation from bare ground where the latent heat comes from the substrate. In either case, the energy loss is part of the surface-energy budget, which affects the atmosphere.

The rate of loss of water by transpiration from vegetation depends on many factors, including vegetation type and density, atmospheric humidity, time of day, season, and the degree of heat and water stress to which the vegetation has been subjected. There has been considerable historical controversy about the dependence of the transpiration rate on soil moisture. A wilting-point value of soil-moisture content has been defined as the limit below which the vegetation permanently wilts and transpiration ceases. This is a convenient concept, but ignores the fact that the moisture content within the root zone is not uniform, and that different coexisting vegetation types have greatly different tolerances for soil dryness. Field capacity is another threshold on the soil-moisture scale, with implications for vegetation. It is defined as the moisture value below which internal drainage ceases. That is, for a soil-moisture content that is less than the field capacity, the soil will retain the moisture and none will drain downward. This is another concept that has gained popularity because of its simplicity rather than its strict accuracy. Some have used the assumption that water is equally available to vegetation for any moisture value above the wilting point. Others have assumed that the vegetation is under stress for wetnesses between the wilting point and field capacity, with a transpiration rate that is dependent on soil moisture, and that only for wetnesses above field capacity is there no longer a stress.

5.2.5 Heat and water-vapor exchange between the surface and the atmosphere

It was mentioned previously that the vertical transfer of sensible heat at the substrate–atmosphere interface occurs through conduction. This takes place within a very shallow layer of atmosphere, called the laminar (nonturbulent) sublayer, having a depth of a few molecules to, at most, a few millimeters. Above this layer, the transfer is through turbulent eddies of air. This turbulence does not contribute to the flux at the surface because the eddies cannot exist there, where the velocity normal to the surface must be zero.

Because all nonradiative transfer of heat at the surface is through conduction, the heat flux can be represented (Eq. 5.12) by the same sort of flux-gradient relationship employed to represent heat transport by conduction within the substrate (Eq. 5.4). A similar expression (Eq. 5.13) can be used for the vapor flux. If it is assumed that the same type of equations can be applied for turbulent transfer as are used for molecular transfer,

the equations can be rewritten as follows with the molecular diffusivities replaced with eddy diffusivities:

$$H = -C_a K_{Ha} \left.\frac{\partial T}{\partial z}\right|_0 = -\rho c_p K_{Ha} \left.\frac{\partial T}{\partial z}\right|_0 \text{ and} \tag{5.12}$$

$$LE = -C_a K_{Wa} \left.\frac{\partial q}{\partial z}\right|_0 = -\rho c_p K_{Wa} \left.\frac{\partial q}{\partial z}\right|_0 . \tag{5.13}$$

Here, C_a is the heat capacity of the atmosphere, c_p is the specific heat at constant pressure of the atmosphere, K_{Ha} and K_{Wa} are the diffusivities of heat and water vapor in the air, respectively, q is specific humidity, and the vertical derivatives are evaluated within the laminar sublayer near the surface.

A challenge to applying these equations is that the exchange coefficients are functions of distance from the surface and static stability, varying by over three orders of magnitude from day to night. Alternative expressions for H and LE can be obtained if we vertically integrate these equations with the assumption that the fluxes do not vary much with height within the first couple of meters. The resulting expressions are

$$H = \rho c_p D_H (T_g - T_a) \text{ and} \tag{5.14}$$

$$LE = \rho L D_W (q_{s,sat}(T_g) - q_a), \tag{5.15}$$

where D_H and D_W are transfer coefficients that are integral functions of K_{Ha} and K_{Wa}, T_g is the temperature of the surface, and T_a and q_a are the temperature and specific humidity, respectively, of the air at a specified level near the surface. The value of the specific humidity at the surface, q_s, is equal to the saturation value, $q_{s,sat}$, at the temperature T_g, of any surface at which evaporation is occurring – water bodies, damp soil, leaf stomata.

Thus, the sensible- and latent-heat fluxes between the substrate and the atmosphere can be represented in terms of the differences between the temperature and humidity at and immediately above the surface. The direction of the fluxes depends on the sign of the difference, and the magnitude of the fluxes depends on the degree of the contrast between the conditions at the two levels. The transfer coefficients are functions of factors that affect the intensity of the turbulence, such as the roughness of the surface, the vertical shear of the horizontal wind from which turbulent energy can be derived, and the vertical lapse rate of atmospheric temperature, which determines whether turbulent energy is available from buoyancy. For example, evaporation rates (LE) are high when the atmosphere is dry (small q_a), the surface is warm (large $q_{s,sat}$) and wet, and the near-surface wind speed is high (producing a large shear, and thus a large transfer coefficient, D_W).

Another way of visualizing the controls on the surface heat flux is through the concept of thermal admittance. Most of the earlier discussion about admittance was in the context of the substrate properties; however, it was pointed out that the admittance of the atmosphere on the other side of the interface is equally important in determining the heat fluxes. This atmospheric admittance is defined as $\mu_a = (k_a C_a)^{1/2} = C_a K_{Ha}{}^{1/2}$, where K_{Ha} is the

eddy diffusivity of Eq. 5.12. For example, suppose that the surface is receiving solar radiation during the day. This heating of a thin layer of substrate and air at the interface will produce a temperature gradient within both the air and the substrate (see Fig. 5.3). The energy not lost by longwave emission and evaporation will be partitioned between sensible-heat fluxes into the atmosphere and the substrate in proportion to the relative admittances of the two media. Say, for example, that the substrate has a very low admittance because of poor thermal conductivity, but the boundary layer has a large admittance because the turbulence is well developed and thus the eddy diffusivity is large. The heat flux into the soil (Eq. 5.4) will thus be small in spite of the large $\partial T_s / \partial z$, but the heat flux into the atmosphere (Eq. 5.12) will be large because the eddy diffusivity, K_{Ha}, is large. Thus, more of the radiant-energy input to the surface will be partitioned to the sensible-heat flux to the atmosphere rather than to the substrate. Alternatively, at night the radiative cooling of the surface draws heat from the air and the substrate in proportion to their admittances. Because calm, near-surface winds and a stable vertical profile of temperature mean that turbulence is weak and the eddy diffusivity is small, the atmospheric admittance is small at night and most of the surface heat lost to space by radiation is provided by the substrate rather than by the atmosphere. Methods of estimating atmospheric and substrate admittances are discussed in Novak (1986).

5.2.6 Horizontal water movement at and below the surface

Water from rainfall or snowmelt that accumulates on the surface too rapidly to infiltrate downward, ponds in the low spots of the substrate and eventually runs off laterally at the surface. When this occurs, the runoff is channeled across the landscape until reaching streams and rivers. The rate of infiltration, which determines the partitioning to runoff, of course depends on the soil type, the density and type of vegetation, the amount of organic litter on the surface, and the soil-moisture content. Some of the excess that runs off laterally will possibly infiltrate at another location. Because runoff is caused by the potential energy of the water, the horizontal redistribution is greatest and occurs most rapidly over steeply sloping terrain.

5.3 Ocean or lake processes that must be modeled

This section will provide only a brief summary of processes at and below a water surface that can affect the atmosphere in model simulations. The reader should be able to distinguish, based on scale, discussions of those processes that are associated with oceans and seas, in contrast to lakes. More-comprehensive discussions of ocean processes can be found in Miller (2007) and Haidvogel and Beckmann (1999). Chapter 16 on climate modeling discusses ocean and sea-ice processes that must be included for simulations on seasonal and longer time scales. As with the land surface, it is not necessary to include all of these processes for all model applications. Section 5.5 will clarify the level of complexity that must be included for different modeling situations.

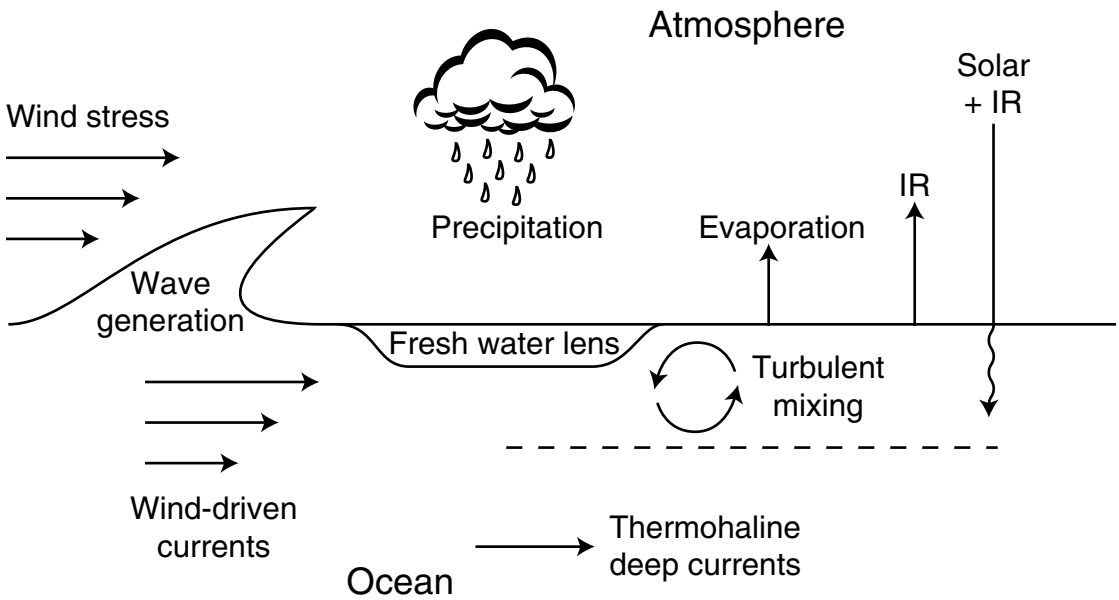

Fig. 5.5 Schematic showing physical processes that are associated with the movement of heat and mass within the ocean. The IR notation refers to infrared radiation.

Figure 5.5 illustrates some of the processes that may be represented, explicitly or through parameterization, in models of the coupled atmosphere–water system. The wind at the surface causes waves, where the wave height is a function of the wind speed and the fetch. In turn, the stress between the atmosphere and the water is a function of the wave height. The surface waves and the subsurface turbulence, caused by the wind stress, mix the water through a layer that is tens to hundreds of meters deep (the mixed layer). The density, which is a function of the temperature and salinity, is relatively uniform in this well-mixed layer. In addition to the depth and intensity of the mixing being functions of the waves and wind speed, they also depend on the density stratification, or stability, of the near-surface water. The more stable the surface water, the weaker is the mixing and the shallower is the mixed layer (analogous to the atmospheric mixed layer). The near-surface stability depends on the vertical distribution of heating from incoming atmospheric radiation, the flux of fresh water from precipitation at the surface, and the mixing of warmer surface water with cooler water below through the turbulence. Precipitation is less dense than saline ocean water, and can remain on the top as a fresh-water lens. This increases the stratification, making it more difficult to mix the less-dense, heated, surface water downward by turbulence. This, in turn, results in higher Sea-Surface Temperatures (SST) associated with the fresh-water lens.

The radiation budget differs from that over a land surface in a number of respects, one of the most important being that the incoming solar and infrared radiation penetrate the medium and distribute the energy over a depth that depends on the water's turbidity. The greatest amount of radiant energy is absorbed near the surface, before the beam loses intensity through attenuation. The turbulence in the ocean distributes this warmer, near-surface

water through the mixed layer. The diurnal variation of surface temperature is significant (Kawai and Wada 2007), but less than that over land because the energy is distributed through a layer by virtue of the penetration of the radiation and the turbulent mixing.

The wind also drives basin-scale near-surface ocean circulations, called gyres. Near coastlines, the Ekman drift associated with the Coriolis force can deflect the water movement away from the coast, causing upwelling that greatly influences water temperatures and the coastal climate.

5.4 Modeling surface and subsurface processes over land

As noted earlier, LSMs can be run as integral components of LAMs and global models, or they can be used autonomously as part of a LDAS, with input from observations instead of the atmospheric-model output. Modeling land-surface processes begins with mapping the types of substrate (e.g., rock, sand, loam) and vegetation (e.g., shrubs, coniferous trees, deciduous trees) over the computational area. A look-up table is then used to provide base values for physical variables, corresponding to the different substrate and vegetation types. Such variables would include substrate thermal conductivity, heat capacity, porosity, albedo, etc., where adjustments are made to variable values that are functions of surface or subsurface moisture. Figure 5.6 shows a schematic of the overall land-surface-modeling process. The landscape-related input variables are provided by the module in the upper left. In the upper right is the input of initial estimates of time-dependent variables such as substrate moisture content and temperature, which vary in both time and space, and are predicted by the LSM. Because these variables are not observed operationally, it is necessary to adjust the estimated values through the use of a LDAS, which requires observed atmospheric variables for forcing. It is necessary for this LDAS to run for months to years, in order to spin up the correct current conditions for the soil-temperature and -moisture profiles. After this spinup period, the LSM and soil state are ready to use for research or operational prediction. See Section 5.4.2 for further discussion of the concept of the LDAS. At the bottom of the figure is an LSM, coupled with an atmospheric model, that has used input from the LDAS to define the land-surface and subsurface conditions at the beginning of the model integration. Once the land-variable profiles are spun up, the LDAS is integrated forward on an hourly basis, as input observations become available, and output is used to initialize the land variables for operational forecasts.

The next subsection reviews land-surface-modeling methods, the second one describes the use of LSMs in LDASs, and the last one discusses how the LSMs are coupled with atmospheric models for weather and climate prediction.

5.4.1 Land-surface models

Now that we have reviewed the array of land-surface and subsurface physical processes that can affect surface–atmosphere interaction, this section will describe how the processes can be represented in a model. There are dozens of different specific formulations for

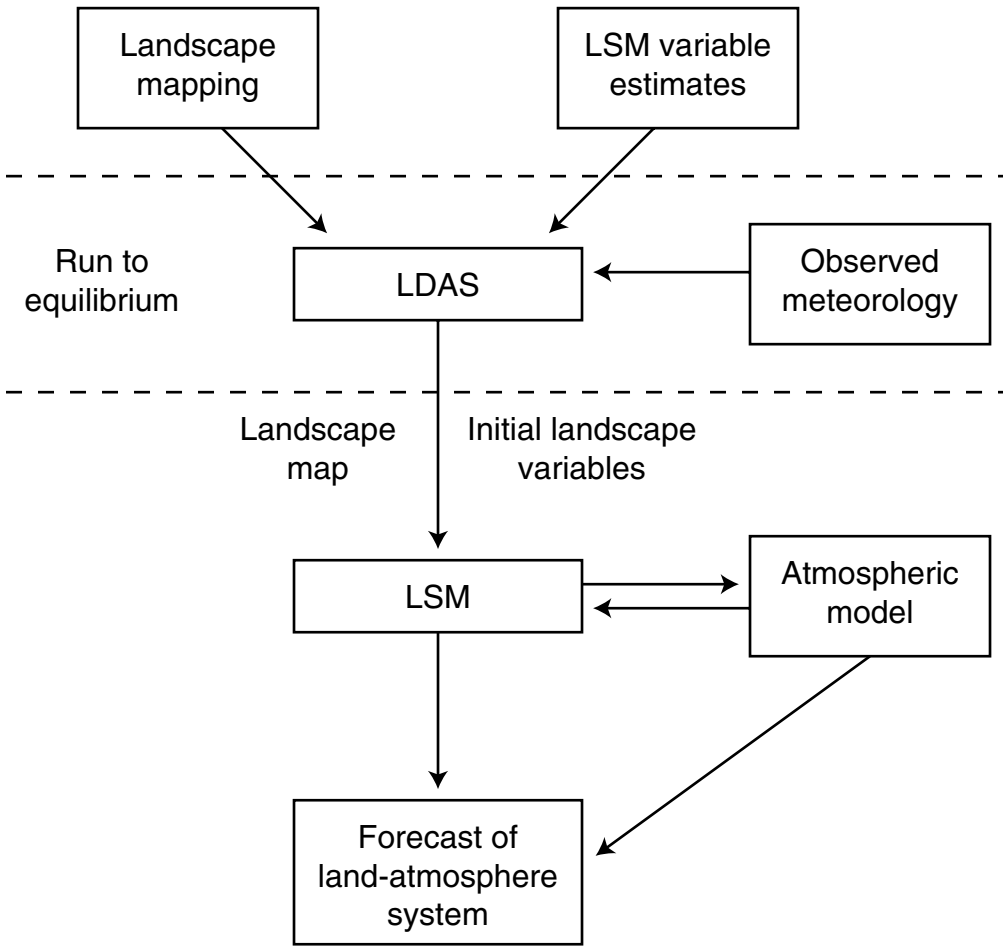

Fig. 5.6 Schematic of the overall land-surface modeling process. At the upper left, the landscape properties (e.g., soil and vegetation type) are defined, and in the upper right a first guess of the vertical profiles of soil moisture and temperature are generated. These data sets are input to a LDAS that is driven by observed atmospheric forcing, and that is integrated forward in time for a historical period of months to years in order to allow the spinup of realistic, current, three-dimensional soil temperature and moisture fields. These conditions can then be used as input to a coupled atmosphere–land modeling system for production of weather forecasts, or they can be used directly for hydrological or other applications.

LSMs. For example, the Project for Intercomparison of Land-surface Parameterization Schemes (PILPS) included 23 schemes (Henderson-Sellers *et al*. 1995, Shao and Henderson-Sellers 1996, Chen *et al*. 1997). These references should be consulted for a summary of the varied computational approaches used in the participating LSMs, and for documentation of the models. The more-complete LSMs represent all the processes depicted in Fig. 5.1, and sometimes more when simulations are on interseasonal and climate time scales. One of the outcomes of the intercomparison was that sophisticated LSMs do not consistently outperform the simpler schemes. The reason for this is that it is

virtually impossible to accurately define values on the local scale for the vast number of physical quantities that are used by some vegetation–soil–hydrology models.

Essentially, the LSM solves numerical (finite-difference) forms of Eqs. 5.1, 5.2, 5.3, 5.6, 5.9, 5.14, and 5.15. The net radiation defined in Eq. 5.2 is calculated as follows.

- The flux of direct solar radiation, Q, at the surface is calculated using the astronomical equations that define the Earth–Sun relationship during the diurnal and seasonal cycles (the elevation and azimuth angles of the incoming solar beam), the slope of the terrain, the attenuation of the solar beam by gases, clouds, and particles in the atmosphere (calculated by a radiation parameterization), and the solar spectral flux at the top of the atmosphere. For climate–time-scale simulations, the solar flux is varied based on known periodicities in the solar output and changes in Earth's orbital parameters.
- The indirect-solar radiation, q, is obtained from a radiation parameterization, using the above information about the direct solar beam, and information about atmospheric particulate and liquid scatterers.
- The albedo, α, is based on the tabulated substrate and vegetation properties of the grid box, as well as the substrate wetness (which affects the albedo). Strictly speaking, the albedo is dependent on the wavelength, the incident angle of the radiation, and the viewing angle, but a single value is usually used as an approximation.
- The upward-propagating infrared energy at the surface is calculated from the time-dependent skin temperature (T_g) of the vegetation and soil, using $I\uparrow = \varepsilon\sigma T_g^4$, where ε is the emissivity and σ is the Stefan–Boltzmann constant.
- The downwelling infrared energy at the surface is calculated from $I\downarrow = \varepsilon I$ (incident), where the incident longwave flux at the surface is provided by the radiation parameterization.

The resulting net radiation is used in Eq. 5.1. The terms in this equation for the sensible (H) and latent (LE) heat-flux exchanges between the surface and the atmosphere are calculated with Eqs. 5.14 and 5.15, respectively. The heat flux between the surface and the uppermost substrate layer (G) is computed with Eq. 5.4, with the surface (skin) temperature (T_g) and the temperature of the uppermost soil layer used to calculate the vertical temperature derivative. Each of these terms in Eq. 5.1 is a function of T_g, which is obtained by iteration.

Within the substrate, temperature change is computed by integrating Eq. 5.6 in time. The water budget for the surface is computed by integration of Eq. 5.3, where the precipitation rate (P) is obtained from the atmospheric model, the loss by evapotranspiration (ET) and lateral runoff (R) are computed using various approaches, and the drainage to deeper layers is computed with flux terms such as in Eq. 5.9. Changes in the soil-moisture content of subsurface layers are calculated by integrating Eq. 5.9.

Some of the major ways in which land-surface parameterizations differ from each other are listed below.

- Land- and sea-ice process modeling
- Vegetation canopy representation
- Runoff calculation and surface routing (results from merger of hydrologic models and LSMs)

- Grid-box partitioning (whether model grid boxes contain a mixture of surface types, or whether the dominant surface type is applied to the entire grid box)
- Groundwater modeling
- Snowpack, snow-cover, snow-albedo treatments
- Dynamic vegetation, multi-layer vegetation canopy representation
- Urban canopy modeling (none, single-layer, multi-layer)
- Irrigation representation (seasonal and daily protocols)
- Frozen-soil treatment

5.4.2 Land-surface models used in land data-assimilation systems

The use of LDASs has two motivations. One is to initialize the land-surface conditions (e.g., soil moisture and temperature) in atmospheric-model integrations. Even though these quantities are forecast by the LSMs that are run with the atmospheric model, they develop forecast errors just as do the atmospheric variables. Therefore, using the forecast values of land-surface variables as initial conditions for a subsequent forecast can result in the accumulation of error associated with model biases. Thus, LDASs are needed in order to provide realistic land-surface initial conditions (IC). The second motivation is to diagnose surface properties that are too difficult or expensive to measure directly. For example, a LDAS can be run for a forest, and the soil moisture and information about the vegetation can be used to estimate wildfire potential in remote areas. And, a LDAS can be run for an agricultural area, and the output used to diagnose regional variations in the soil-temperature and -moisture profiles that affect crop growth. Or, it can be run for a watershed, and the analyzed soil moisture used as input to a flash-flood forecasting system.

An example of a global LDAS is the Global Land Data Assimilation System (GLDAS, Rodell *et al*. 2004) developed by the US NOAA and NASA. It merges ground- and space-based measurements, which can be used as input to any of three LSMs: Mosaic (Koster and Suarez 1996), the Common Land Model (Dai *et al*. 2003), and Noah (Chen *et al*. 1996, Koren *et al*. 1999). Table 5.1 lists the input and output variables for GLDAS. The atmospheric-forcing variables in the left column are estimated based on observations, these data are used as input to an LSM, and the LSM diagnoses the output variables on the right. The GLDAS has basic grid-increment options of 0.25°, 0.5°, 1.0°, 2.0°, and 2.5°. Higher-resolution, mesoscale LDASs are used for regional applications, but their operation and purpose is the same as on larger scales. These are run using typical mesoscale grid increments of 1–10 km. Chen *et al*. (2007) report on the WRF-based High-Resolution Land Data Assimilation System (HRLDAS), which employs the Noah LSM. Reanalysis systems, described in Chapter 16, also often provide land-surface conditions as part of the archived output, but these are not the same as LDASs because the LSM input is from the model and not observations.

When an LDAS is used for model initialization, it is typical to use the exact same LSM, use the same input data (e.g., substrate properties), and employ identical computational grids for both the LSM in the model and the LSM in the LDAS. This avoids the problem that it is challenging to translate soil-moisture and temperature profiles from one LSM (in the LDAS) to another (in the forecast model) because of different basic assumptions and

Table 5.1 Forcing and output fields for the GLDAS

Required forcing fields	Output fields
Precipitation	Surface albedo
Downward shortwave radiation	Canopy transpiration
Downward longwave radiation	Soil moisture in each layer
Near-surface air temperature	Snow depth, fractional coverage, and water equivalent
Near-surface specific humidity	Plant canopy surface-water storage
Near-surface wind vector	Soil temperature in each layer
Surface pressure	Average surface temperature
	Surface and subsurface runoff
	Bare soil, snow, and canopy surface-water evaporation
	Latent, sensible, and ground heat flux
	Snow phase-change heat flux
	Snowmelt
	Net surface shortwave and longwave radiation
	Aerodynamic conductance
	Canopy conductance
	Snowfall and rainfall

Source: From Rodell *et al.* (2004).

formulations, and different grid structures. For rapidly adjusting atmospheric variables, modest conversion errors would be reconciled quickly. However, LDASs can require many months to reach an equilibrium, after being initialized with erroneous soil-temperature and -moisture profiles.

5.4.3 Land-surface models coupled with atmospheric models

When used this way, the LSM is an integral component of the entire modeling system, with the atmospheric and land-surface components integrated together and communicating at every time step. The LSMs are employed in both weather-prediction and climate-prediction models, and with LAMs and global models. For climate prediction, more degrees of freedom are needed because a changing climate will lead to the evolution of the vegetation species and density. For real-data simulations or forecasts, the land-surface variables in the LAMs are generally initialized using an LDAS, a described in the previous section.

5.5 Modeling surface and subsurface processes over water

At a minimum, the lower boundary of the model atmosphere over water must have the roughness, temperature, ice-coverage, and salinity (which affects saturation vapor pressure) specified. This approach of specifying such lower-boundary quantities over water suffices for short-range forecasts or simulations. An exception exists when hurricanes are being modeled, because the high wind speed produces intense vertical mixing, rapidly leading to a negative anomaly in the SST that must be represented in the simulation. Thus, incorporation of ocean boundary-layer mixing and the resulting SST change into model simulations has been shown to improve hurricane-intensity forecasts (e.g., Bao *et al*. 2000).

In general, for forecasts of longer than a week or two, variables such as water temperature and ice cover should be calculated internal to the atmospheric-model simulation. This requires the use of ocean-circulation models and sea-ice models. Even though it is not the purpose of this section to provide details on ocean-circulation and wave modeling, it is worth mentioning the methods that are used. As described in Chapter 16, for simulation of the Intergovernmental Panel on Climate Change (IPCC) climate scenarios, and for initial-value simulations of years to decades, relatively physically complete ocean models are used. For interseasonal predictions, sometimes ocean models are run separately from the atmospheric model. For weather prediction and research, on smaller scales in maritime environments, coupled ocean–atmosphere LAMs are used. For example, the COAMPS is a LAM that has been used for a wide variety of applications for processes in the open sea and in littoral zones (e.g., Pullen *et al*. 2006). Similarly, Bao *et al*. (2000) have coupled the MM5 mesoscale atmospheric model, an ocean-wave model, and a version of the Princeton Ocean Model for regional-process studies.

Sometimes wave-height forecasts are needed, and this requires that atmospheric-model forecasts be used as input to wave-height models. Because the output from the wave-height model does not typically get fed back to the atmospheric model (i.e., the coupling is one way), wave models are discussed in Chapter 14, which is about special-application models.

At land–sea boundaries, it is especially important that the model have grid points defined correctly in terms of whether they are land or water points. That is, the land–sea mask, as it is called, which defines the coastline, must be accurate. This requirement sounds trivial, but the complex configuration of many coastlines means that sometimes grid points or observation points are defined to be on the wrong side of the coast. Thus, a land observation may be erroneously compared with a water grid point, and even though the points are close to each other, the model solution verifies poorly for obvious reasons.

5.6 Orographic forcing

The forcing of the atmosphere by orography is important on all scales, from the global to the mesoscale. Thus, except for models that are used for pedagogical applications, or those that employ less-than-complete physics to allow for simpler interpretation of the results in

studies of physical processes or numerical methods, virtually all models allow for variable orography. Gridded data sets of terrain elevation are available with a variety of horizontal resolutions, with grid increments ranging from tens of meters to tens of kilometers. There are two considerations when deciding upon the best degree of smoothness to use to define the lower-boundary elevation in a model. If there is too much variability of the elevation in the 2–4 Δx wavelengths, this will be reflected in energy in these wavelengths in the model solution, which can require heavier filtering to avoid the development of nonlinear instability. However, one of the motivations for using high horizontal resolution in a model is to permit the development of atmospheric features that result from small-scale forcing at the lower boundary. Thus, the terrain data set should be of as high a resolution as possible, while avoiding the wavelengths that will generate troublesomely short wavelengths in the model solution.

Any terrain-elevation data set is going to show some effects of smoothing relative to the actual terrain, with elevation maxima that are less than observed, and elevation minima that are higher than observed. That is, valleys will be less deep than they should be, and mountains will be less tall than they should be. The use of such smoothed data sets in models has implications for the accurate representation of processes that depend on the orographic extremes. For example, the amplitude of standing planetary waves, the drag of mountains on the atmosphere, and the effectiveness of the blocking of tropospheric synoptic-scale features are dependent upon the height of the lower-boundary obstacles. Indeed, it has been argued that the large-scale flow responds to an envelope that somewhat intersects the mountain peaks, rather than to the mean elevation of the mountains and valleys. That is, the height of terrain obstacles should be preserved in models, regardless of the smoothness of the terrain data set. This elevation-preserving topography is called *envelope topography.* Wallace *et al*. (1983) first tested this approach with the ECMWF model, because it was noted that model solutions showed persistent negative height biases over mountain ranges. They enhanced the orographic elevation by adding to the grid-box average value an increment that was proportional to the subgrid-scale variance in the true orography. Their tests showed forecast improvement for longer lead times, but a degradation for shorter times. Other approaches have been used to define the envelope orography. For example, Mesinger *et al.* (1988) defined the grid-box-average elevation as the tallest actual value for the area. Other applications of this approach have led to mixed results (e.g., Tibaldi 1986, Lott and Miller 1997, Georgelin *et al.* 2000). Even though this method has conceptual appeal, its implementation should be thoroughly evaluated in particular applications. For satisfying the particular need of improved mountain drag, Catry *et al.* (2008) suggest an alternative to the use of envelope orography in the French ARPEGE/ALADIN model.

An example is shown in Fig. 5.7 of how horizontal resolution can affect the ability of a model to correctly define the orography with which the atmosphere interacts. Shown is the terrain elevation for two different model horizontal resolutions, for the same region of complex orography in the southwestern USA. In one, the grid increment is 30 km, and in the other it is 3.3 km. No methods for defining envelope orography were employed. The coarser-resolution grid defines the significant regional topographic features with only a couple of grid points, and any atmospheric response to the orography on these scales is going to be filtered strongly by the model.

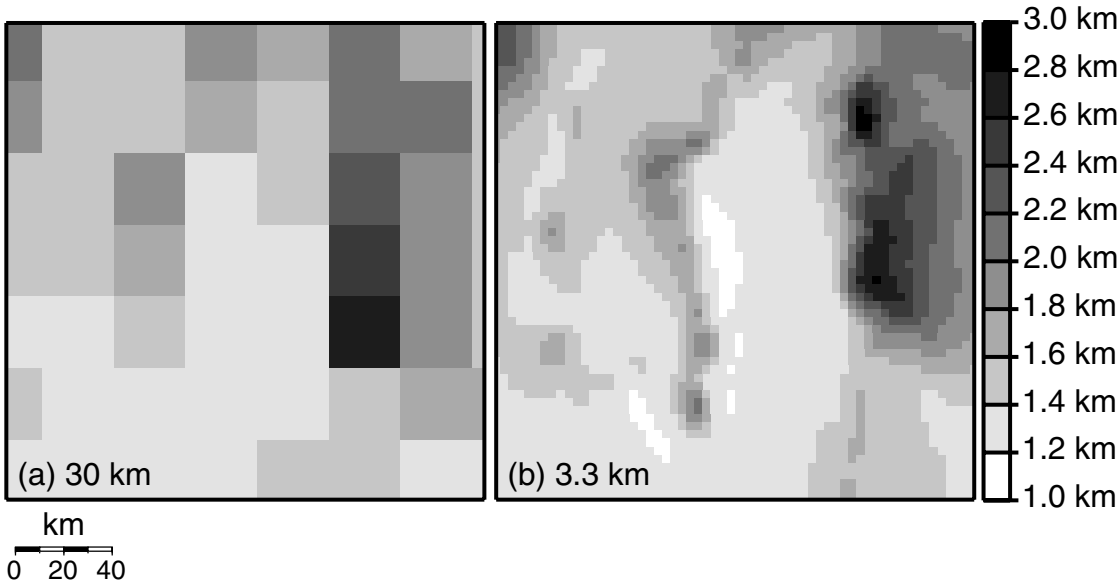

Fig. 5.7 The terrain elevation (see gray shades on the right) for two different model horizontal resolutions, for the same region of complex orography in the southwestern USA. In (a) the grid increment is 30 km and in (b) it is 3.3 km.

5.7 Urban-canopy modeling

There exists a number of modeling approaches for representing the dynamic and thermodynamic effects of urban areas on the atmosphere. One is to employ a Computational Fluid Dynamics (CFD) model that explicitly represents the effect of each building or other structure on the atmosphere. However, as described in Chapter 15, these models are very computationally expensive to use. In contrast to such fine-scale modeling, what is commonly needed is simply a way of representing the bulk effects of built-up areas on mesoscale processes. The simplest approach is to employ standard LSMs by defining the surface properties so that they approximate the artificial surface conditions in cities. For example, roughness length can be increased to represent the drag from buildings; albedo can be decreased to account for the existence of asphalt pavement, dark rooftops, and the trapping of shortwave radiation in street canyons; the heat capacity and thermal conductivity of the substrate can be elevated above standard values for asphalt and concrete to account for heat storage in building walls; the substrate water capacity can be decreased to reflect the prevalence of impermeable surfaces; and the green-vegetation fraction can be reduced. Liu *et al*. (2006) used this approach to successfully simulate urban–rural boundary-layer differences for Oklahoma City, USA. However, other methods need to be used to represent more-complex processes that are associated with the existence of buildings and non-natural substrates. Tools to accomplish this are called Urban Canopy Models (UCM, also known as urban canopy parameterization), which represent the model grid-cell-averaged effect of the building structures on the dynamics and thermodynamics. Such UCMs

parameterize the aggregate effects of the urban morphology, but individual buildings and street canyons are not explicitly represented (Masson 2000, Kusaka *et al.* 2001, Martilli *et al.* 2002). Many UCMs consider the geometry of buildings and roads to represent the radiation trapping and wind shear in the urban canopy. Such an approach requires detailed three-dimensional, urban land-use data sets, and the input of a number of parameters that define the urban geometry, where these parameters need to be calibrated for each individual city. Because of the cost of mapping the three-dimensional geometries of tens of thousands of structures, these data sets are not available for many cities. Figure 5.8 illustrates one of the many factors that can be included in a UCM; in this case it is the shadowing that results from a particular configuration of structures. Two different sun angles are illustrated, where the smaller zenith angle (θ_z) shades one side of a building and part of the street, while the larger one also shades part of the building on the opposite side of the street canyon.

Most UCMs to date have been single-layer parameterizations. That is, even though the vertical effects of buildings are represented, the fluxes of heat, moisture, and momentum are defined at the bottom boundary of the lowest atmospheric layer in the model. In contrast, multi-layer UCMs allow direct interaction between buildings and multiple layers in

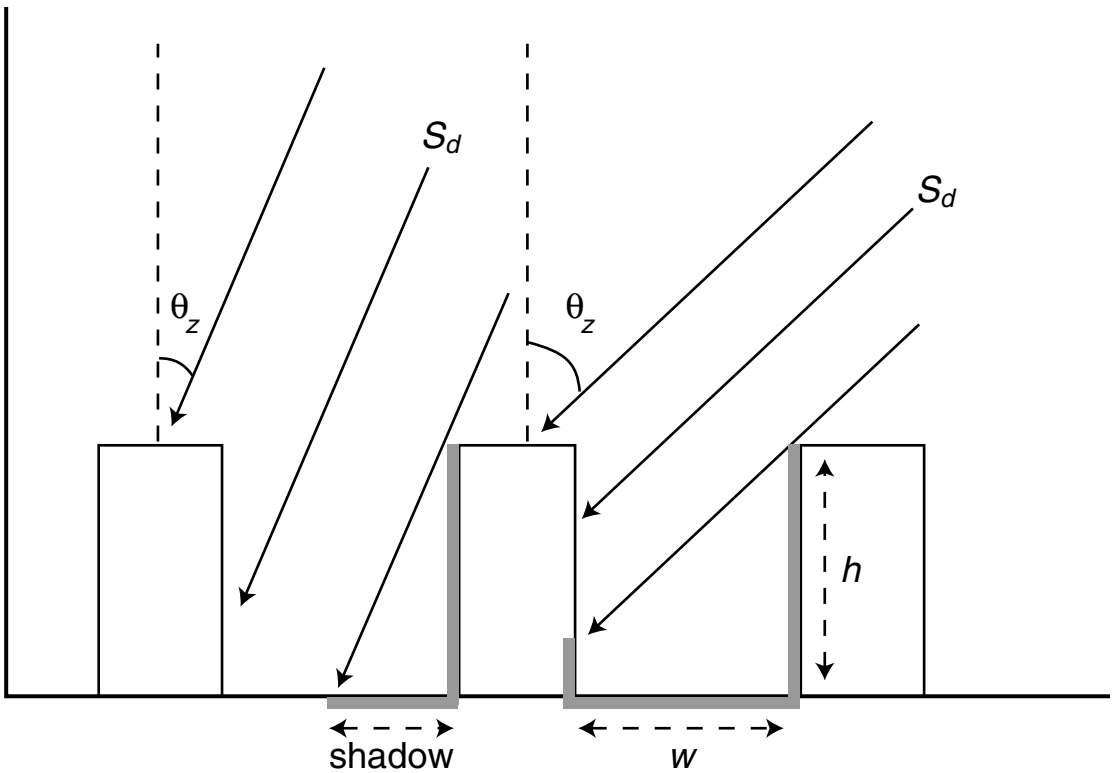

Fig. 5.8 Illustration of how UCMs must use the three-dimensional morphology of urban landscapes to calculate the illumination of the surface of the street canyon and the sides of the buildings. Similarly, this geometry is required to calculate the longwave radiation trapping in the street canyons. Shown are the direct solar radiation (S_d) and the zenith angle (θ_z). Adapted from Kusaka *et al.* (2001).

the atmospheric model (even though obviously the buildings are not explicitly resolved). See Kusaka *et al.* (2001), Chin *et al.* (2005), Kondo *et al.* (2005), Holt and Pullen (2007), and Martilli (2007) for further discussion of multi-level UCMs.

5.8 Data sets for the specification of surface properties

As noted before, there are two general kinds of landscape variables. One defines the substrate type, and vegetation type and density, as a function of location. There are a number of national and regional data sets that represent surveys of these properties. For example, for the USA, the Geological Survey's Earth Resources Observing System (EROS) 1-km dataset (Loveland *et al.* 1995) defines vegetation type, and the State Soil Geographic (STATSGO) 1-km database defines soil type (Miller and White 1998). The EROS data set can need significant correction based on field reconnaissance.

The second kind of variable represents the time and space variability of the specific physical properties of the substrate and vegetation, such as temperature and soil-moisture content for the substrate, and the leaf-area index or the green vegetation fraction for the vegetation (which can vary as a function of season and antecedent rainfall). The variables of both kinds need to be defined for any model application over land. The LDASs described above can be used to define values for the substrate physical properties. For example, the GLDAS data set provides the variables listed on the right of Table 5.1. When the same land-surface parameterization is used in both GLDAS and the LSM that is coupled with the atmospheric model, no soil-moisture conversion is required. Numerous satellite-based methods are used to define the state of the vegetation (e.g., Gutman and Ignatov 1998).

For water, surface-temperature analyses are available from a variety of sources. For example, the NCEP Version 2.0 global SST data set (Reynolds *et al.* 2002) is defined on a $1° \times 1°$ grid and updated daily. Also, the Real-Time Global (RTG) analysis (Thiebaux *et al.* 2003) from the Marine Modeling and Analysis Branch of NCEP produces a two-dimensional variational analysis of data from buoys, ships, and satellites over the preceding 24 hours. The product is incorporated into the NCEP North American mesoscale Model (NAM) and the global forecast model at ECMWF. Since 2001, the RTG analysis has been available daily on a grid with pixel size of 0.5 deg latitude and longitude. In 2005, a 1/12-deg product became available. There is also an optimum interpolation SST analysis from NOAA. It is available weekly, and with a pixel size of 1/3 deg. The product uses *in-situ* and satellite SST observations, and incorporates a weekly median ice concentration.

SUGGESTED GENERAL REFERENCES FOR FURTHER READING

Bonan, G. (2008). *Ecological Climatology.* Cambridge, UK: Cambridge University Press.

Hillel, D. (1998). *Environmental Soil Physics*. San Diego, USA: Academic Press.

Martilli, A. (2007). Current research and future challenges in urban mesoscale modelling. *Int. J. Climatol.*, **27**, 1909–1918.

Oke, T. R. (1987). *Boundary Layer Climates*. London, UK: Methuen.
Stensrud, D. J. (2007). *Parameterization Schemes: Keys to Understanding Numerical Weather Prediction Models*. Cambridge, UK: Cambridge University Press.
Stull, R. B. (1988). *An Introduction to Boundary Layer Meteorology.* Dordrecht, the Netherlands: Kluwer Academic.

PROBLEMS AND EXERCISES

1. Why are microclimate conditions less extreme when high soil diffusivities prevail?
2. Miller (1981) describes the following situation. When a cold air mass (−17 °C) moved over an area near Leningrad, the surface flux was 45 W m^{-2} over frozen bare soil with an admittance of 1000 J m^{-2} K^{-1} $s^{-1/2}$, but was only 15 W m^{-2} over an adjacent snow-covered surface with an admittance of about 330 J m^{-2} K^{-1} $s^{-1/2}$. Explain these measurements in the context of the definition and meaning of admittance.
3. List the ways in which land-surface properties in urban areas differ from those elsewhere, and explain how these differences can be incorporated into LSMs in order to reasonably represent urban land-surface effects.
4. Perform a literature search on the use of coupled ocean–atmosphere LAMs, and describe why it can be important to represent regional ocean processes in forecasts having weather time scales.
5. How would the choice of the depth of the substrate layer that is modeled depend on whether the model is being used for weather, interseasonal, or long-term (multi-decadal) climate prediction?
6. Show mathematically that the depth to which the annual cycle's temperature wave penetrates into the substrate is about 14 times greater than the penetration depth of the diurnal cycle's temperature wave.
7. Based on physical arguments, describe what specific vegetation effects need to be modeled to account for the vegetation's influence on the surface-energy budget, and the atmosphere.